Journal of Research in Engineering and Computer Sciences
August 2023, Vol. 1, No. 3, pp. 43-66

Analysis of the Influence of the Water/Graphene Nanofluid as Working Fluid on the Thermal Performance of Finned Heat Pipes Used in Air Conditioning

Élcio Nogueira

1. Department of Mechanic and Energy, State University of Rio de Janeiro, Brazil

Abstract:
This is a theoretical analysis of the influence of fractions of graphene nanoparticles associated with distilled water as a working fluid in a heat exchanger used in an air conditioning system for operating rooms. The heat exchanger consists of a set of finned heat pipes. Theoretical results are confronted with experimental results for water as the working fluid. The analysis is restricted to the evaporator since the nanoparticles do not influence the results in the condenser heat exchanger. The thermal efficiency method is applied to obtain the results. The analysis presents results for air velocity, Nusselt number for air, overall evaporator heat exchange coefficient, evaporator Nusselt number, evaporator thermal effectiveness, and the air outlet temperature. It was determined that the influence of fractions of graphene nanoparticles is not significant on the evaporator heat exchanger analyzed. Despite this, it is observed that smaller fractions of nanoparticles have a greater influence on thermal performance and there is an upper limit for volume fractions.

Keywords: Finned heat pipes, water/graphene nanofluid, air conditioning, boiling heat transfer correlations, thermal efficiency method.

INTRODUCTION

The objective is to apply the analytical thermal efficiency method to analyze the influence of graphene particles on the performance of the heat pipe system in the evaporator of the heat exchanger studied by Ragil Sukarno [1]. The Figures below show the heat pipe system in the evaporator and condenser, and how they are in a staggered configuration in rows of 4 pipes. The original working fluid is water and has a saturation temperature of 27°C.

The system used in the experiment carried out for the thermal analysis of the heat exchanger consists of sets of 12, 24, and 36 finned heat pipes, as shown in Figure (1.a), Figure (1.b) and Figure (1. c). The experiment was carried out by Ragil Sukarno et al. [1], who used the effectiveness method (ε-NTU) for global analysis of the heat exchanger. The finned heat pipe heat exchanger (FHPHE) has a staggered configuration consisting of three, six, and nine rows of heat pipes. The air inlet temperature in the evaporator ranges from 30.0°C to 45°C. The airflow ranges from 0.05 kg/s to 0.095 kg/s.

Nandy Putra et al. [2] experiment with heat recovery using finned heat pipes, with water as the working fluid, in an air conditioning system. They analyze the influence of the number of heat pipes, inlet temperature, and inlet air velocity. They determine that finned heat exchanger performance strongly depends on air velocity and that higher inlet velocity enables better performance.

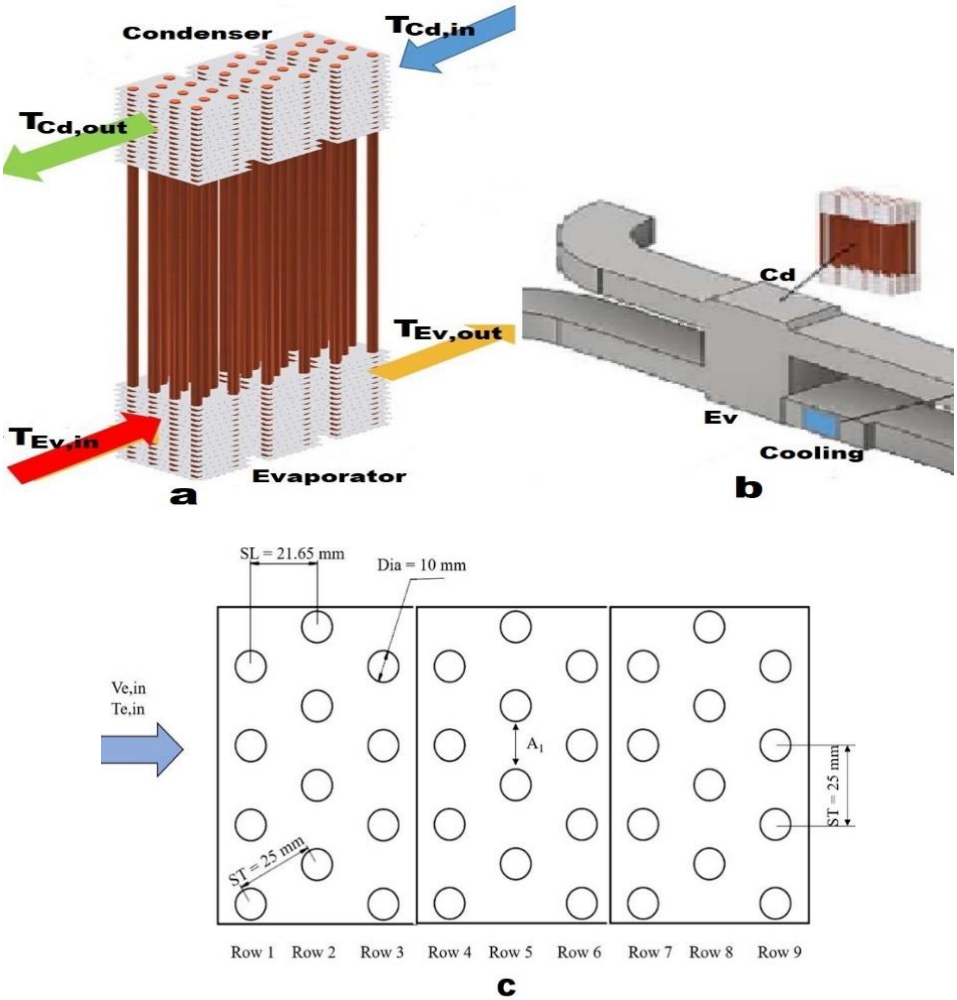

Figure (1. a) represents the set of finned heat pipes [1]; Figure (1. b) represents the evaporator (pre-cooling), conventional cooling, condenser (energy recovery), and air circulation pipes [1]; Figure (1. c) schematically represents the set of finned heat pipes arranged in the heat exchanger shell [1].

Grzegorz Górecki et al. [3] study a small air-conditioning system consisting of individually finned heat pipes using R404 refrigerant as the working fluid. Theoretical-experimental work makes it possible to conclude that individual fins are an alternative to conventional heat exchangers and that they are less susceptible to deformation and easy to replace and clean.

H. Jouhara et al. [4] uses a finned tube heat exchanger consisting of multiple passes. The theoretical-experimental study aims at heating water using heated air, that is, recovery of residual energy. They use two theoretical methods for determining thermal quantities and comparing them with experimental results. It is a global implementation of the heat exchanger, and the methods used by them were the Log Mean Temperature Difference Method (LMTD) and the Effectiveness Method (ε-NTU). They report the significant importance of the Reynolds number in thermal performance.

Khaled Elsaid et al. [5] present a discussion related to the use of graphene as a nanofluid component with a focus on thermophysical properties. They argue that nanofluids using graphene have higher thermal conductivity than most nanofluids using metallic oxides and present a table of properties for comparison. However, they point out that there are major

challenges related to its use. They cite cost, stability, higher values for density and viscosity, environmental impacts, and preparation methods. They conclude that such challenges require careful investigation.

Naser Ali [6] studies characteristics related to graphene, such as thermophysical properties, and dispersion stability. It presents values for density, thermal capacity, thermal conductivity, and viscosity, in graphic form, for a nanofluid composed of water and graphene, with percentage values of volume fraction equal to 0.01%, 0.05%, and 0.10%. He argues that a feasibility study of the presented nanofluid is necessary before being used in real applications. Emphasizes cost, performance evaluation, and environmental impact aspects. It also analyzes the use of surfactants related to the stability of the nanofluid and concludes that stability of 45 days can be reached when using higher-weight surfactants.

The performance of thermosiphons can be improved with the use of nanofluids, as argued by A. Kamyar et al. [7]. They present a study to corroborate their statements and use two nanofluids using water mixed with Al_2O_3 and $TiSiO_4$ nanoparticles, with volume fractions equal to 0.01%, 0.05% and 0.07%. The results presented demonstrate that there is a reduction in thermal resistance and an improvement in the performance of the thermosiphons. They emphasize that the boiling coefficient increases with the use of nanoparticles in thermosiphons and, as a numerical argument, they use the Merit number that makes it possible to determine the relative effect of the properties of the nanofluid. However, they consider that the performance of thermosiphons depends on particle size, particle type, bubble nucleation size, and base fluid.

Agnieszka Kujawska et al. [8] state that the performance of the condenser is not influenced by the nanofluids used in the heat pipe and that the performance analysis should be concentrated on the evaporator. They analyze the surface tension and contact angle of silica and graphene oxide nanofluids and argue that nanoparticles tend to deposit on the surface of the evaporator during the boiling process. This deposit alters the conditions in the wall and in the region close to it, and the effect this may have on the nanofluid properties is unknown. It is known, however, that changes in surface tension and wettability affect the boiling regime. The study presents numerical results for the surface tension of graphene oxide before and after the boiling process, with water as the base fluid. They also analyze the influence of surfactants on the surface tension associated with the nanofluid. They conclude that graphene has surface tension and contact angle similar to water, when in small concentrations and state, citing references, that the impact of graphene oxide on heat transfer capacity is not related to surface tension or wettability. However, they add, more research is needed to determine the influence of the use of nanofluids in thermosyphons at the boiling process, and that the studies carried out are rarely associated with real applications, especially in low-pressure devices.

Amir Akbari et al..[9] state that the use of nanofluids related to an increase in nucleated boiling has aroused great interest. They carried out an experimental study conducted under atmospheric pressure to compare the effects of graphene nanoplatelets and multi-walled carbon nanotubes on the heat transfer coefficient associated with pool boiling and the critical heat flux. They verified that nanoparticles with percentage concentrations in weight equal to 0.01, 0.05, and 0.1% altered the heat transfer coefficient and the critical heat flux, about deionized water. Concentrations above 0.01% by weight decreased the heat transfer coefficient and increased the critical heat flux. Furthermore, they experimentally demonstrated that the thermal conductivity of nanofluids and

the functionalization method (non-covalent and covalent) directly affect the heat transfer coefficients and the critical heat flux.

Jaqueline Barber et al. [10] published a review related to recent advances in pool boiling and convective boiling related to the use of nanofluids. The review work focused on the improvement and degradation in the nucleate boiling heat transfer coefficient and critical heat flux and concluded that there are conflicting data published in the literature presented in tabular form. They found that most of the work reports that the deposition of nanoparticles on the surface of the heat exchanger is related to an increase in the critical heat flux with the use of nanofluids.

K. N. Shukla et al. [11] present experimental work with a cylindrical copper heat pipe filled with different working fluids. They performed tests with deionized water, and nanofluids composed of silver-aqua and copper-water. They found a 14% increase in heat pipe efficiency with the use of nanofluids compared to deionized water as the working fluid. They observed an increase in the thermal conductivity of nanofluids with 0.1% by weight of nanoparticles. They find that nanoparticles can create several active nucleation sites, enabling an increase in heat transfer by boiling, with a consequent decline in the temperature profile.

Kapilan Natesan and Shashikantha Karinka[12] argue that the use of energy in its various forms is vital for the development of any country. They add that it is one of the most used devices in heat transfer applications and that any effective improvement of heat exchange between fluids brings benefits. They claim that the solid particles have higher thermal conductivity than the usual working fluids used in heat pipes and can improve the efficiency of heat exchangers. They mention that graphene-based nanoparticles have high thermal conductivity, low erosion, and enable an increase in the heat transfer rate. This improvement in heat transfer can lead to equipment downsizing in different types of applications. In this sense, the review highlights the advantages of using graphene, for example, in electronic devices.

Mohammed Salah Hameed [13] recognizes that there are four correlations frequently used to simulate nucleate boiling and that each of them is differentiated by the variables used in its implementation. With the objective of improving the precision in the determination of the boiling heat transfer coefficient, they develop a generalized empirical correlation that satisfies a wide range of experimental data available in the literature. They use the least squares multiple regression techniques to determine a correlation that allows minimum deviation. They test the correlation developed by the linear and non-linear programming solution and using a wide range of literature data presented by Rohsenow, Forster and Zuber, Forster and Greif, and Gupta and Varshney.

Suriyawong et al. [14] present a study where they developed a new correlation for predicting the nucleate pool boiling heat transfer coefficient of TiO_2-Water nanofluids for low concentrations. The proposed correlation considers several relevant factors. They use data obtained from studies that show correlations associated with nanofluid properties and develop a correlation that predicts results with good accuracy for the copper surface but with poor accuracy for the aluminum surface.

Élcio Nogueira [15] applied the second law of thermodynamics through the concepts of thermal efficiency, thermal effectiveness, and thermal irreversibility in a shell and tube heat exchanger utilizing a water-ethylene glycol associated with fractions of nanoparticles. Volume fractions

equal to 0.01, 0.10, and 0.25 were considered for analysis for nanoparticles of Ag and Al_2O_3. He concluded that, when the Reynolds number is relatively small in a laminar regime, high effectiveness, associated with high thermal irreversibility, leads to heat transfer rates that approach the maximum possible.

Élcio Nogueira [16] states that the thermal efficiency method, associated with viscous irreversibility and the thermodynamic Bejan number, enables analysis of the optimization of heat exchangers. It applies the method to the cooling of machine oil in a heat exchanger with external fins associated with the tubes. He includes spherical nanoparticles of Boehmite Alumina in the analysis, concluding that the inclusion of nanofluid presents a significant improvement in thermal performance, associated with an increase in viscous dissipation, and a decline in the Bejan number.

Élcio Nogueira [17] analyzes the influence of the thermal performance of a shell and tube-type condenser, with water and aluminum oxide (Al_2O_3) nanoparticles flowing into the tube. The principles parameters used to analyze the thermal performance are thermal efficiency and thermal effectiveness, and the results demonstrate that efficiency is high and that the effectiveness can be increased by introducing fractions of nanoparticles in the water.

METHODOLOGY

The formulation below, Equations (1) – (91) is related to the thermal performance of the heat exchanger analyzed by Ragil Sukarno et al. [1], represented through Figures 1.a, 1.b and 1.c. Graphene volume fractions are represented by the parameter ϕ which ranges from 0.001 to 0.100.

$$T_{sat} = 27.0\,^{o}C \;\; fixed \tag{1}$$

$$T_{airin} = 30\,^{o}C \;\; default,\; 30^{o}C \le T_{airin} \le 45^{o}C \tag{2}$$

$$T_W = T_{airin} \;\; by\ definition \tag{3}$$

T_{sat} is the saturation temperature of the working fluid, T_{airin} is the air inlet temperature, T_W is the surface temperature of the heat pipe.

$$\phi = 0.01 \;\; default,\; 0.001 \le \phi \le 0.100$$

ϕ is the volume fraction of the nanofluid

$$k_{air} = 6.9174418610^{-5} Tair_{in} + 0.02462173663 \tag{4}$$

$$\mu_{air} = 1.9548362110^{-5} + 2.73505803910^{-9} Tair_{in} + 2.30958747910^{-10} Tair_{in}^2 - 4.50588235310^{-13} Tair_{in}^3 \tag{5}$$

$$Cp_{air} = 1003.728948 + 0.06727399886 * Tair_{in} + 3.56591836710^{-6} Tair_{in}^2 + 8.22222222210^{-7} Tair_{in}^3 \tag{6}$$

$$\rho_{air} = 1.219135515 - 0.002152770329 Tair_{in} - 3.6404747910^{-7} Tair_{in}^2 + 1.70588235310^{-9} Tair_{in}^3 \quad (7)$$

$$\nu_{air} = \frac{\mu_{air}}{\rho_{air}} \quad (8)$$

$$\alpha_{air} = \frac{k_{air}}{\rho_{air} Cp_{air}} \quad (9)$$

$$\mathrm{Pr}_{air} = \frac{\nu_{air}}{\alpha_{air}} \quad (10)$$

Equations (4-10) represent the properties of air at the air inlet temperature.

$$k_W = 0.5521904762 + 0.002561507937 T_W - 1.8720238110^{-5} T_W^2 + 5.90277777810^{-8} T_W^3 \quad (11)$$

$$Cp_W = 4217.8 - 3.412833333 T_W + 0.109375 T_W^2 - 0.0016890625 T_W^3 + 1.34375\,10^{-5} T_W^4 - 4.088541667\,10^{-8} T_W^5 \quad (12)$$

$$\rho_W = 1002.676071 - 0.06559821429 T_W - 0.003582589286 T_W^2 \quad (13)$$

$$\nu_W = 1.787666667\,10^{-6} - 5.532222222\,10^{-8} T_W + 9.82708333310^{-10} T_W^2 - 8.96527777810^{-12} T_W^3 + 3.17708333310^{-14} T_W^4 \quad (14)$$

$$\mu_W = \rho_W \nu_W \quad (15)$$

$$\alpha_W = \frac{k_W}{\rho_W Cp_W} \quad (16)$$

$$\mathrm{Pr}_W = \frac{\nu_W}{\alpha_W} \quad (17)$$

Equations (11-16) represent the properties of water at the heat pipe.

$$P_{sat} = 216.7691429 - 5.927342857 T_{sat} + 0.04774285714 T_{sat}^2 \quad (18)$$

P_{sat} is the saturation pressure of the working fluid.

$$\nu_l = 0.001585485714 - 1.83190476210^{-5}T_{sat} + 1.95714285710^{-7} T_{sat}^2 - 6.666666667\,10^{-10}T_{sat}^3 \tag{19}$$

$$\rho_l = \frac{1}{\nu_l} \tag{20}$$

$$\nu_V = 21.45466571 - 0.3398517143T_{SAT} + 0.001419714286T_{sat}^2 \tag{21}$$

$$\rho_v = \frac{1}{\nu_v} \tag{22}$$

Equations (19-22) represent the properties of the saturated liquid and saturated vapor in the heat pipe.

$$h_l = 2.184 + 4.2124T_{sat} \tag{23}$$

$$h_v = 1.540666667T_{sat} + 2521.596667 \tag{24}$$

$$h_{lv} = h_v - h_l \tag{25}$$

h_{lv} represents the latent heat of vaporization.

$$NHP = 12\ default; 12 \le NHP \le 36 \tag{27}$$

NHP is the number of heat pipes associated with the heat exchanger.

$$NFin = 30\ default;\ \ 0 \le NFin \le 30 \tag{28}$$

$NFin$ is the number of fins per heat pipe.

$$NHP_{byrows} = 4 \tag{29}$$

NHP_{byrows} is the number of heat pipes per row.

$$Nrows = \frac{NHP}{NHP_{byrows}},\ \ 3 \le Nrows \le 9 \tag{30}$$

$Nrows$ is the number of rows in the heat exchanger.

$$Vair_{inlet} = 1.5\ m/s\ default\ ;\ 1.5 \le Vair_{inlet} \le 2.5 \tag{31}$$

$Vair_{inlet}$ is the air velocity at the evaporator inlet.

$$\dot{m}_{air} = 0.050\ kg/s\ default;\ 0.050 \le \dot{m}_{air} \le 0.095 \tag{32}$$

$\dot{m}_{air}$ is the mass flow rate of air.

$$TEv_{in} = T_{airin};\ 30.0^{o}C \le TE_{in} \le 45.0^{o}C \tag{33}$$

$$\sigma_{Water} = 0.07275\left(1 - 0.002\left(368.15 - 291.15\right)\right) \rightarrow \textit{valid for water} \tag{34}$$

σ_{Water} is the surface tension associated with water.

$$r = 0.33 \tag{35}$$

$$C_{sf} = 0.015 \tag{36}$$

$$C_{sf}^{*} = 1503 \tag{37}$$

$$l^{*} = \sqrt{\left(\frac{\sigma_{Water}}{g(\rho_l - \rho_v)}\right)} \tag{38}$$

l^{*} is the characteristic length.

$$q'' = \mu_W h_{lv} l^{*} \left(\frac{1}{Csf}\right)^{0.33} Pr_W^{\ 1/r} \left(\frac{\sigma_{Water} \Lambda T_{sat}}{h_{lv}}\right)^{1/r} \tag{39}$$

q'' is the heat flux associated with the boiling process based on the equation obtained by Rhosenow[18].

$$h_{boil} = 1.39\left(\frac{k_W}{l^{*}}\right)\left(\frac{q''\rho_W Cp_W l^{*}}{\rho_W h_{lv} k_W}\right)^{0.7}\left(\frac{\rho_l}{\rho_v}\right)^{0.21}\left(\frac{\mu_W Cp_W}{k_W}\right)^{-0.21} \rightarrow \text{valid for water} \tag{40}$$

h_{boil} Equation (40), an expression developed by Gupta and Varshney, is the heat transfer coefficient associated with the boiling process valid for water [13].

$$\rho_{Grap} = 3000\ kg/m^3 \tag{41}$$

$$k_{Grap} = 2500\ W/(mK) \tag{42}$$

$$Cp_{Grap} = 711\ J/(kgK) \tag{43}$$

$$\mu_{nano} = (1-\phi)^{-2.5}\mu_W \tag{44}$$

$$\rho_{nano} = \phi\rho_{Grap} + (1-\phi)\rho_W \tag{45}$$

$$Cp_{nano} = \frac{\phi\rho_{Grap}Cp_{Grap} + (1-\phi)\rho_W Cp_W}{\rho_{nano}} \tag{46}$$

$$k_{nano} = [\frac{k_{Grap} + 2k_W + 2(k_{Grap} - k_W)(1+0.1\phi)^3\phi}{k_{Grap} + 2k_W - 2(k_{Grap} - k_W)(1+0.1\phi)^2\phi}]k_W \tag{47}$$

$$\mu_{nano} = \rho_{nano}\nu_{nano} \tag{48}$$

$$\alpha_{nano} = \frac{k_{nano}}{\rho_{nano}Cp_{nano}} \tag{49}$$

$$\Pr_{nano} = \frac{\nu_{nano}}{\alpha_{nano}} \tag{50}$$

$$\sigma_{nano} = 0.0726505555 - 1.621336444d-5*Tsat - 1.367231268d-6*Tsat**2.0 \tag{51}$$

σ_{nano} is the surface tension associated with nanofluid [7].

$$\varepsilon = 0.210^{-6} \tag{52}$$

ε is the surface roughness [15].

$$h_{boil} = 28.85\,Pr_{nano}^{0.59}(\frac{q''\varepsilon}{\mu_{nano}h_{lv}})^{0.70}(\varepsilon^2 g(\frac{\rho_{nano} - \rho_v}{\sigma_{nano}}))^{0.16}(\frac{k_{nano}}{\varepsilon(\phi + 0.001)}) \rightarrow \text{valid for nanofluid} \tag{53}$$

h_{boil} Equation (53) is the heat transfer coefficient associated with the boiling process valid for nanofluid [14].

$$\Delta T_{Evsat} = TEv_{in} - T_{sat} \tag{54}$$

$$D_{ext} = 10.3\,10^{-3}\ m \tag{55}$$

$$D_{\text{int}} = 10.0\,10^{-3}\ m \tag{56}$$

D_{ext} is the outer diameter of the heat pipe. D_{int} is the inner diameter of the heat pipe.

$$kW = 401.0\,W/(mK) \tag{57}$$

kW is the thermal conductivity of the heat pipe material (copper).

$$LEv = 160.0\,10^{-3} \tag{58}$$

LEv is the length of the evaporator.

$$LEv_H = N_{Rows}\frac{LEv}{9.0} \tag{59}$$

LEv_H is the horizontal length of the heat exchanger.

$$t_{Fin} = 0.105\,10^{-3} \tag{60}$$

t_{Fin} is the thickness of the fins.

$$k_{Fin} = 235.0 \tag{61}$$

k_{Fin} is the thermal conductivity of the fin material.

$$Sp_{Fin} = 2.0\,10^{-3}\ by\ definition \tag{62}$$

Sp_{Fin} is the distance between fins.

$$LEv_{effec} = LEv - (NFin\,t_{Fin} + 4\pi D_{ext} Sp_{Fin}) \tag{63}$$

LEv_{effec} is the effective length of the evaporator.

$$Dh_{EV} = \frac{4\,LEv_H\ LEv_{effec}}{2(LEv_H + LEv_{effec})} \tag{64}$$

Dh_{EV} is the hydraulic diameter of the evaporator.

$$\mathrm{Re}_{Ev} = \frac{4\dot{m}_{air}}{\pi Dh_{Ev}\mu_{air}} \tag{65}$$

Re_{Ev} is the Reynolds number associated with the evaporator.

$$A\sec_{Ev} = \frac{\dot{m}_{air} Dh_{Ev}}{\mathrm{Re}_{air}\ \mu_{air}} \tag{66}$$

$A\sec_{Ev}$ is the cross-sectional area associated with the evaporator.

$$V_{Ev} = \frac{\dot{m}_{air}}{A\sec_{Ev}\ \rho_{air}} \tag{67}$$

V_{Ev} is the air velocity in the evaporator.

$$ST = 25.010^{-3} \tag{68}$$

$$SL = 21.6510^{-3} \tag{69}$$

ST and SL are lengths associated with the set of heat pipes (Figure 1.c).

$$Vair_{\max} = \frac{ST}{SL - Dext} Vair_{inlet} \tag{70}$$

$Vair_{\max}$ is the maximum air velocity in the evaporator.

$$Atr_{EvFin} = NFin\, LEv_{H}\ LEv \tag{71}$$

Atr_{EvFin} is the heat rock area associated with fins.

$$Atr_{EvHP} = NHP\, \pi D_{ext} (LEv - NFin\, Sp_{Fin}) \tag{72}$$

Atr_{EvHP} is the heat exchange area associated with the heat pipes.

$$A_{EvTotal} = Atr_{EvFin} + Atr_{EvHP} \tag{73}$$

$A_{EvTotal}$ é a área de troca de calor total no evaporador.

$$Nu_{Ev} = F\, 0.71 \mathrm{Re}_{Ev}^{0.5}\, \mathrm{Pr}_{Ev}^{0.36} \left(\frac{\mathrm{Pr}_{Evair}}{\mathrm{Pr}_{EvSurf}}\right)^{0.25} \tag{74}$$

Nu_{Ev} is the Nusselt number associated with the evaporator, where F=0.98 by definition.

$$h_{Ev} = \frac{Nu_{Ev} k_{air}}{Dh_{EV}} \tag{75}$$

h_{Ev} is the convection heat exchange coefficient.

$$mL_{EvFin} = \sqrt{\frac{2h_{Ev}}{k_{Fin} t_{Fin}}} LEv_H \tag{76}$$

mL_{EvFin} dimensionless parameter associated with the fins.

$$\eta_{EvFin} = \frac{\mathrm{Tanh}(mL_{EvFin})}{mL_{EvFin}} \tag{77}$$

η_{EvFin} is the efficiency associated with fins.

$$\beta_{Ev} = \frac{Atr_{EvFin}}{A_{Total}} \tag{78}$$

β_{Ev} is the ratio between the heat exchange area of the fins in relation to the total area.

$$\eta'_{EvFin} = \beta_{Ev}\, \eta_{EvFin} + (1 - \beta_{Ev}) \tag{79}$$

η'_{EvFin} is the effective efficiency associated with the set of fins.

$$Uo_{Ev} = \frac{1}{\frac{1}{h_{boil}} + \frac{D_{ext} - D_{int}}{kW} + \frac{1}{\eta'_{EvFin} h_{Evair}}} \tag{80}$$

Uo_{Ev} is the overall heat transfer coefficient associated with the evaporator.

$$C_{Air} = \dot{m}_{air} Cp_{air} \tag{81}$$

$$C_{Ev} = C_{air} \tag{82}$$

C_{Air} is the heat capacity of air.

$$NTU_{Ev} = \frac{Uo_{Ev} A_{EvTotal}}{CEv} \tag{83}$$

NTU_{Ev} is the number of thermal units associated with the evaporator.

$$Fa = \frac{NTU\sqrt{1+C^{*2}}}{2} \quad for\ cross-flow \tag{84}$$

Fa is a dimensionless parameter called "Analogy of Fins", associated with the efficiency method [16-18]. $C^* = \frac{C_{min}}{C_{max}} = 0$ to the evaporator ($C_{max} \to \infty$).

$$\eta_T = \frac{tanh(Fa)}{Fa} \tag{85}$$

η_T is the thermal efficiency associated with the heat exchanger.

$$\varepsilon_T = \frac{1}{\frac{1}{\eta NTU} + \frac{1+C^*}{2}} \tag{86}$$

ε_T is the thermal effectiveness associated with the heat exchanger.

$$Fa_{Ev} = \frac{NTU_{Ev}}{2} \tag{87}$$

$$\eta_{TEv} = \frac{tanh(Fa_{Ev})}{Fa_{Ev}} \tag{88}$$

$$\varepsilon_{TEv} = \frac{1}{\frac{1}{\eta_{TEv} NTU_{Ev}} + \frac{1}{2}} \tag{89}$$

$$\dot{Q}_{Ev} = \frac{C_{Ev}\Delta T_{Evsat}}{\frac{1}{\eta_{TEv} NTU_{Ev}} + \frac{1}{2}} \tag{90}$$

$\dot{Q}_{Ev}$ is the rate of heat transfer in the evaporator.

$$TEv_{out} = TEv_{in} - \frac{\dot{Q}_{Ev}}{C_{Ev}} \tag{91}$$

TEv_{out} is the outlet temperature of the air in the evaporator.

RESULTS AND DISCUSSION

The results presented below are related to the following parameters for analysis of the formulated problem: the number of heat pipes, the number of fins per heat pipe, air flow rate, air inlet temperature, and graphene volume fraction. The quantities of interest obtained in the analysis were the air velocity in the evaporator, the global heat transfer coefficient, the number of thermal units associated with the evaporator, the effectiveness of the evaporator, and the outlet temperature in the evaporator.

Figure 2 presents theoretical and experimental results[1] for air velocity in the evaporator, as a function of mass airflow rate. The parameters that vary are the number of heat pipes and the number of fins per heat pipe. The air velocity decreases with the increase of heat pipes and increases with the number of fins per heat pipe, that is, the area of the fins has a significant influence on the air velocity. The theoretical results are below the maximum experimental velocity value and the experimental evaporator velocity results are between the valid results for 12 and 24 heat pipes. There is, therefore, theoretical-experimental consistency in the results obtained.

Figure 3 shows values for the overall heat transfer coefficient, with air mass flow rate and graphene nanoparticle volume fraction as parameters. An increase in the coefficient is observed with the increase in the number of fins, and with the imposition of nanoparticles in the working fluid, with a volume fraction equal to 0.01%.

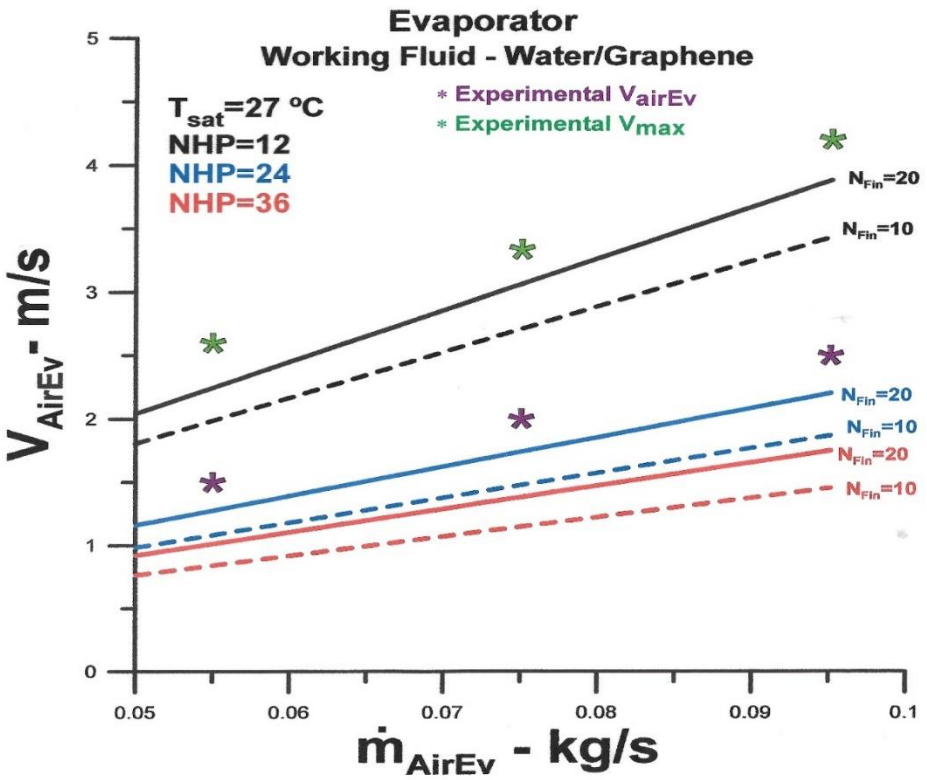

Figure 2: Evaporator air velocity versus mass air flow rate

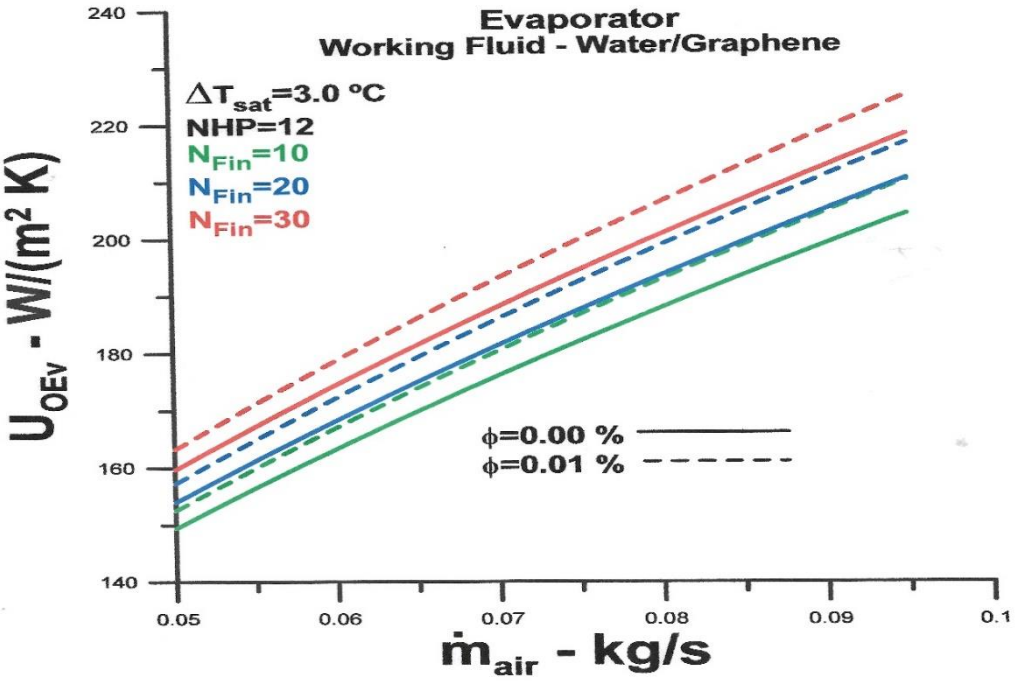

Figure 3: Evaporator Overall heat transfer coefficient versus mass air flow rate

Figure 4 shows that the number of thermal units in the evaporator grows with the number of fins and with the volume fraction of the nanofluid. The influence of nanoparticles, with a volume fraction equal to 0.01%, is more significant when there is an increase in the number of fins per heat pipe, that is when there is an increase in the heat exchange area. However, even for a larger number of fins, the relative difference between results with and without nanoparticles is small.

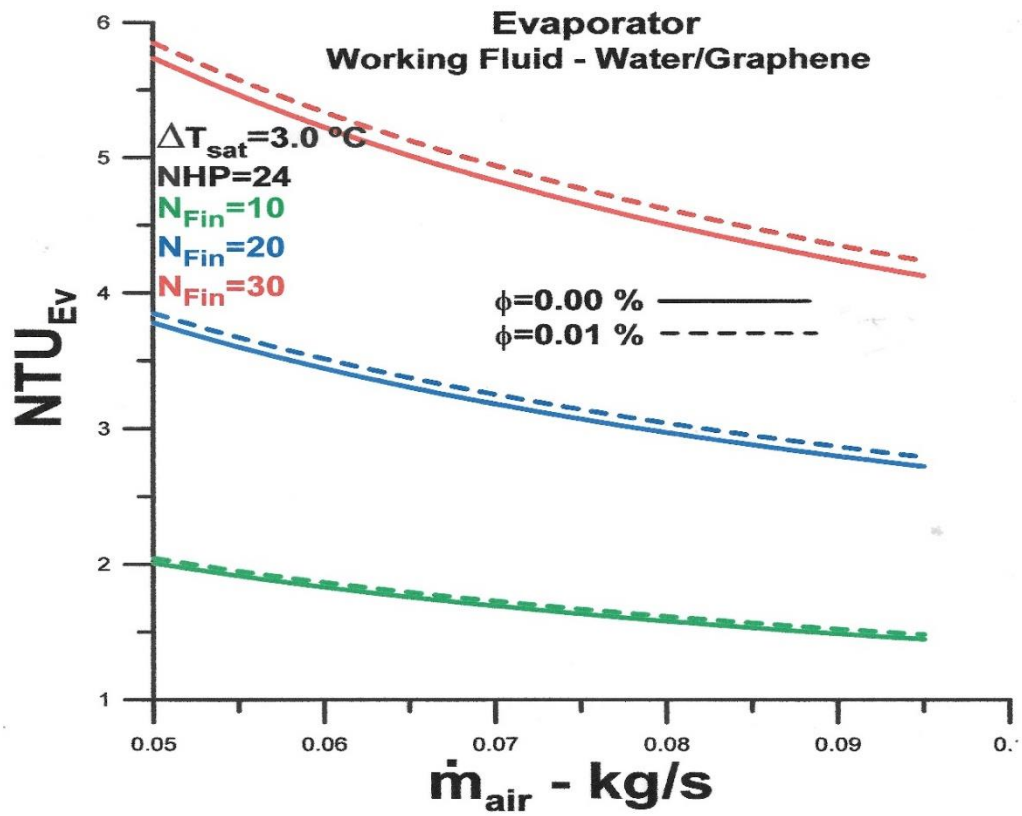

Figure 4: Evaporator number of thermal units versus mass air flow rate

Figure 5 presents results for effectiveness as a function of air mass flow rate and nanoparticles volume fraction, ϕ =0.01. Effectiveness decreases with increasing mass airflow rate. The effectiveness reaches a value very close to the maximum for NHP=24 and N_{Fin}=30, and there is no difference between with and without nanofluid. However, a slight difference can be observed when NFin=10. In practical terms, there is no advantage in using heat pipe values above 24, with 30 fins.

Figure 6 shows theoretical and experimental results for thermal effectiveness, with variation in air inlet temperature and ϕ =0.01. Effectiveness grows with the number of heat pipes and with the number of fins. When comparing situations with and without graphene nanoparticles, a slight increase in effectiveness is observed for lower inlet temperature values. However, the difference becomes almost imperceptible for a larger number of fins. Experimental results [1] are consistent with values obtained through the theoretical procedure.

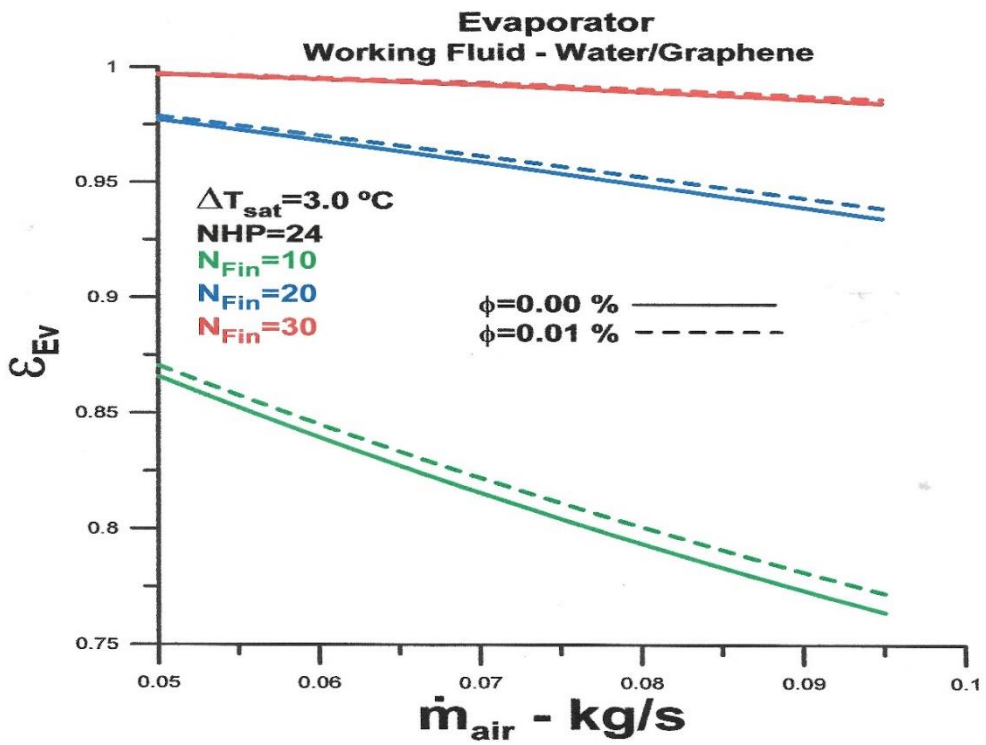

Figure 5: Thermal effectiveness number versus mass air flow rate

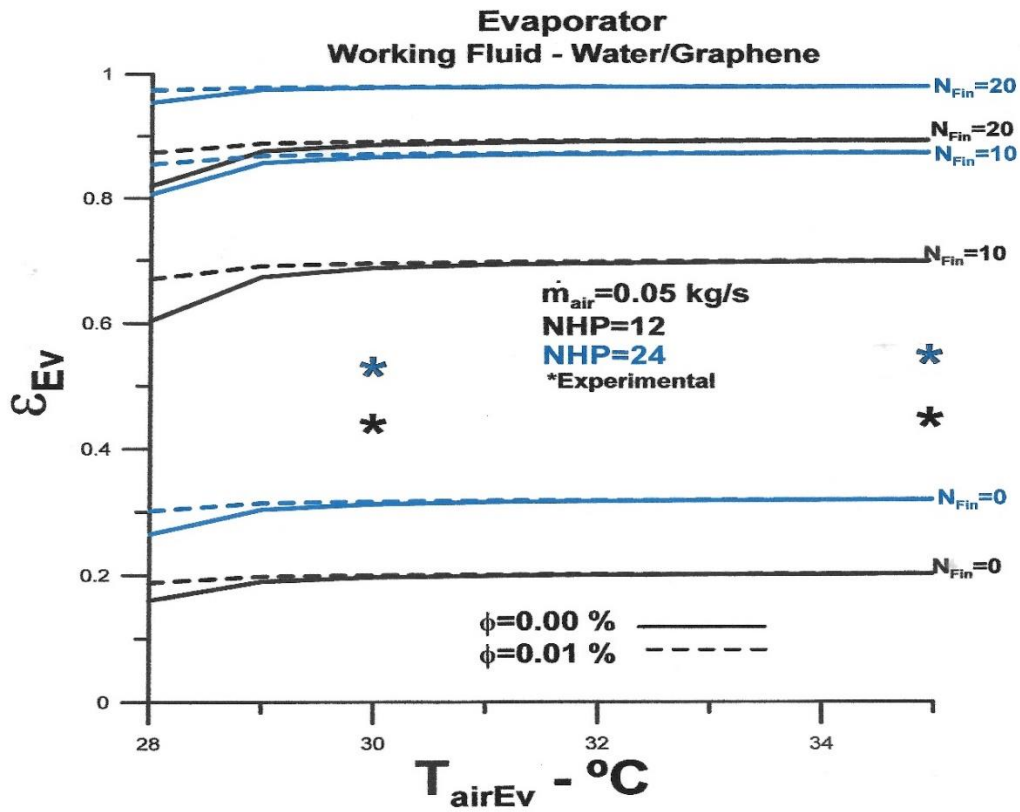

Figure 6: Evaporator thermal effectiveness versus inlet air temperature

The effectiveness versus volume fraction of the nanofluid is shown in Figure 7. Again, the effectiveness grows with the number of heat pipes and with the number of fins. However, there is no graphically perceptible variation in the effectiveness value in the analyzed volume fraction range. This result indicates that there is a saturation in the volume fraction value, that is, for the smallest volume fraction, equal to ϕ =0.01, the effectiveness has reached its highest possible value and there is no advantage in increasing the volume fraction. The questions raised by these results are: 1. Is there an advantage in decreasing the volume fraction value? 2. If so, what is the physical factor that causes the observed saturation, even for a low number of fins?

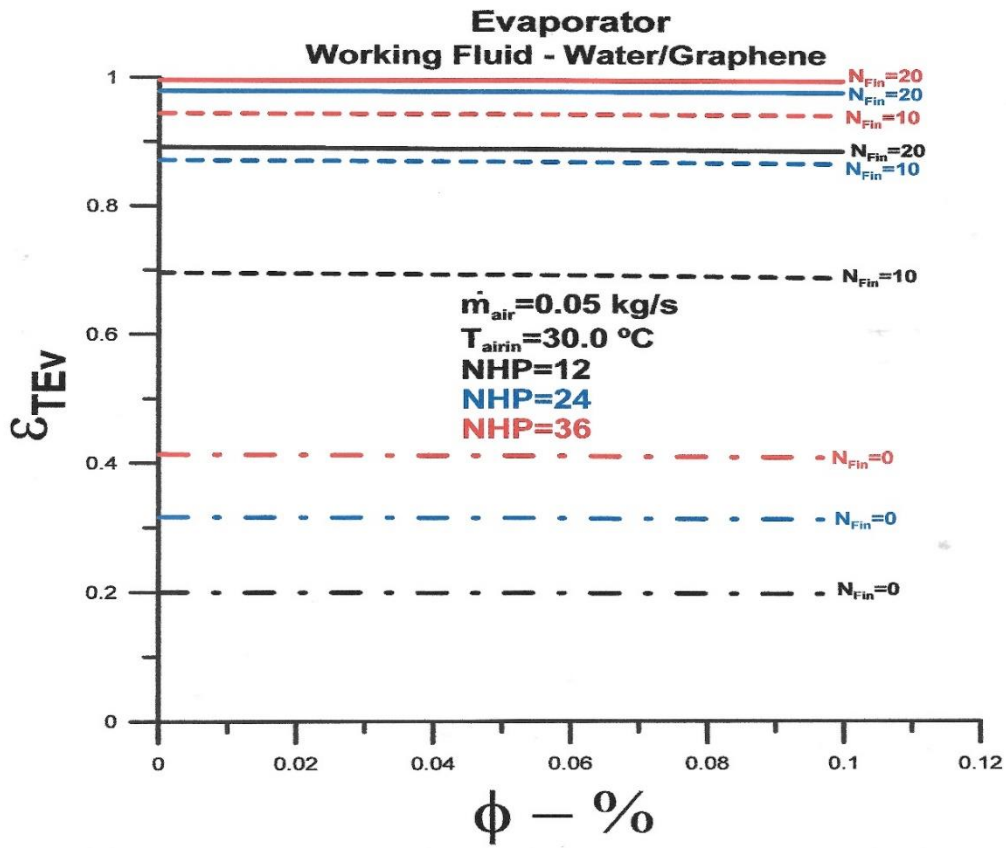

Figure 7: Evaporator thermal effectiveness versus nanofluid volume fractions

In order to try to answer the first question, values for effectiveness with lower values of fraction in volume are presented, in Figure 8. The results obtained are conclusive and demonstrate that lower values of fraction in the volume of the nanofluid allow higher values for effectiveness and that the value ϕ =0.01 is very close to the saturation point. Another interesting factor in the results presented in Figure 8 is that there is also a minimum limit for the volume fraction and that ϕ =0.005 is close to the lower limit for the analyzed configuration. Regarding the second question above, we can speculate, as there is evidence in the literature, that a possible cause for lower heat exchange performance lies in the deposition of nanoparticles on the heat pipe surface, thus increasing the thermal resistance.

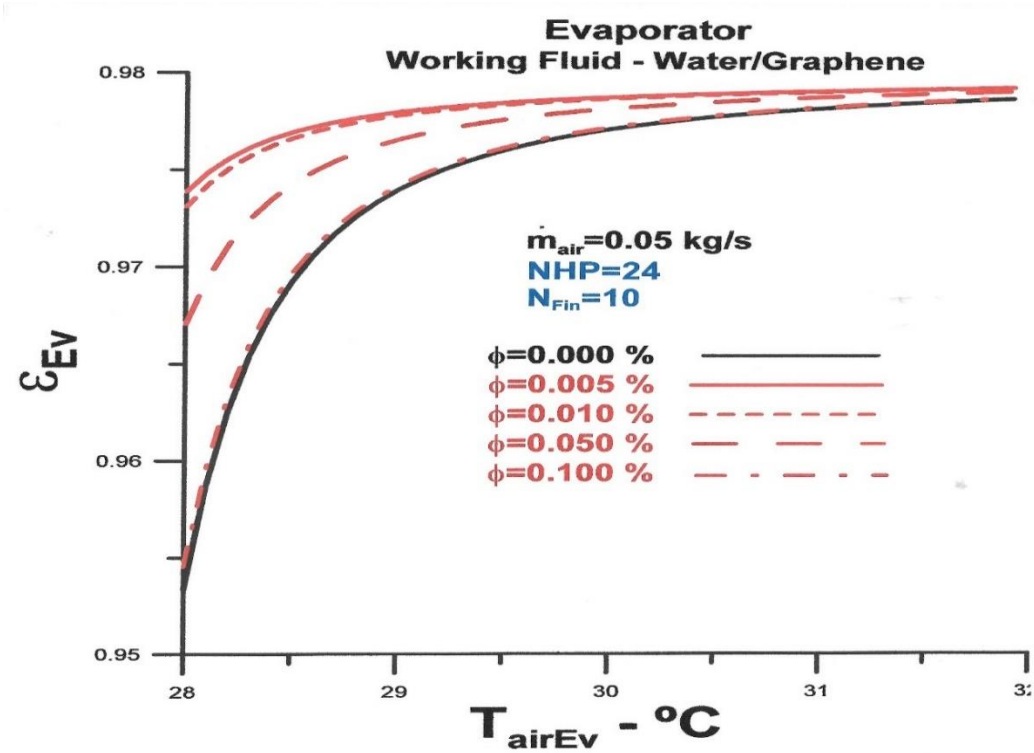

Figure 8: Evaporator thermal effectiveness versus inlet air temperature with nanofluid volume fractions as parameter

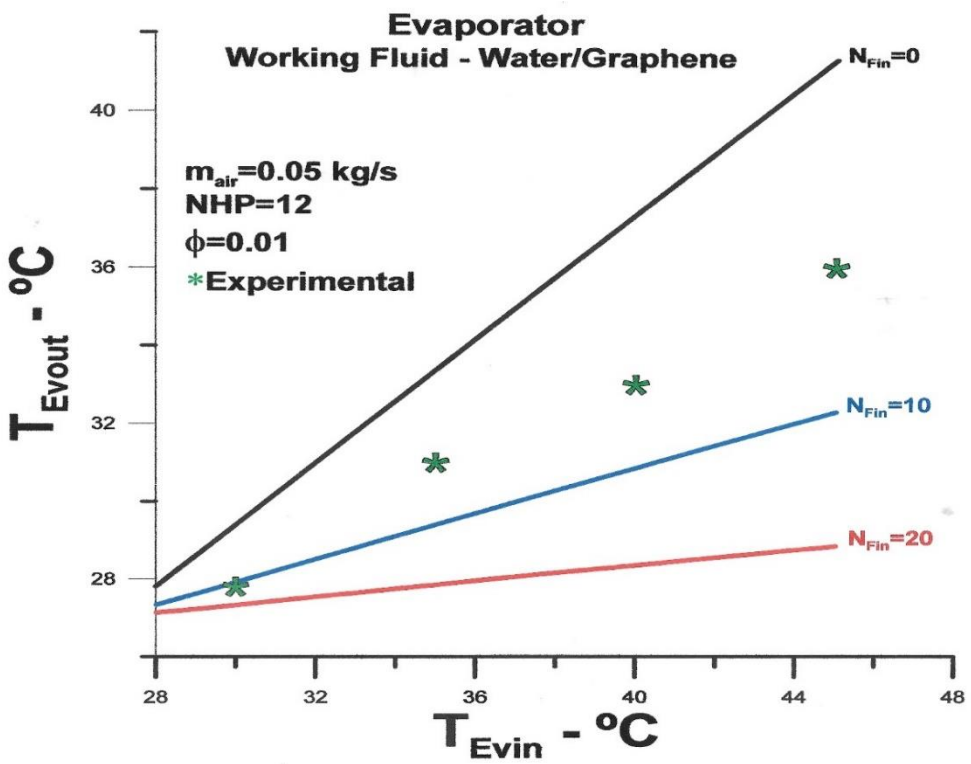

Figure 9: Outlet air temperature versus inlet air temperature

As expected, the results shown in Figure 9 corroborate the results obtained in Figure 5. The theoretical results in Figure 9 are associated with the volume fraction ϕ =0.01. Lower values for the outlet temperature of the air in the evaporator can be observed with the increase in the

number of heat pipes and fins. The experimental results [1] demonstrate consistency with the theoretical procedure.

Results from Figure 10 corroborate the results from Figure 7, as greater effectiveness lowers outlet temperature.

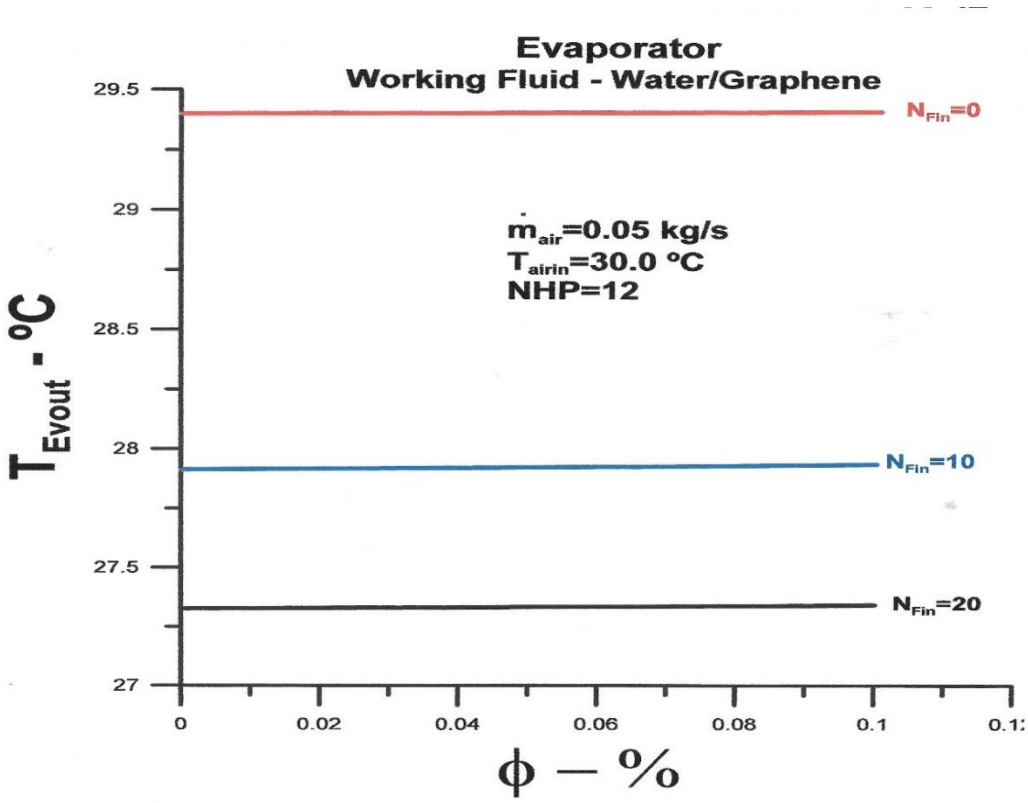

Figure 10: Outlet air temperature versus nanofluid volume fractions

Figures 11, 12, and 13 present results for outlet temperature for numbers of heat pipes respectively equal to 12, 24 and 36. The mass flow rates analyzed are 0.050 kg/s and 0.075 kg/s, with variations in volume fraction of 0.001 to 0.080. The results reinforce what has already been observed, that is, a smaller volume fraction allows a lower air outlet temperature. Although the values obtained for the three analyzed situations did not vary significantly, they demonstrate the importance of the number of heat pipes, associated with the number of fins. Furthermore, the data in Figure 13 demonstrate how the influence of the nanoparticle fraction in the working fluid occurs.

As already mentioned in the introduction, the evaluation of the role of nanofluids associated with heat pipes requires further studies that contribute to the various factors that affect thermal performance, especially for applications where the pressure field and the heat exchanged between the fluids are relatively low.

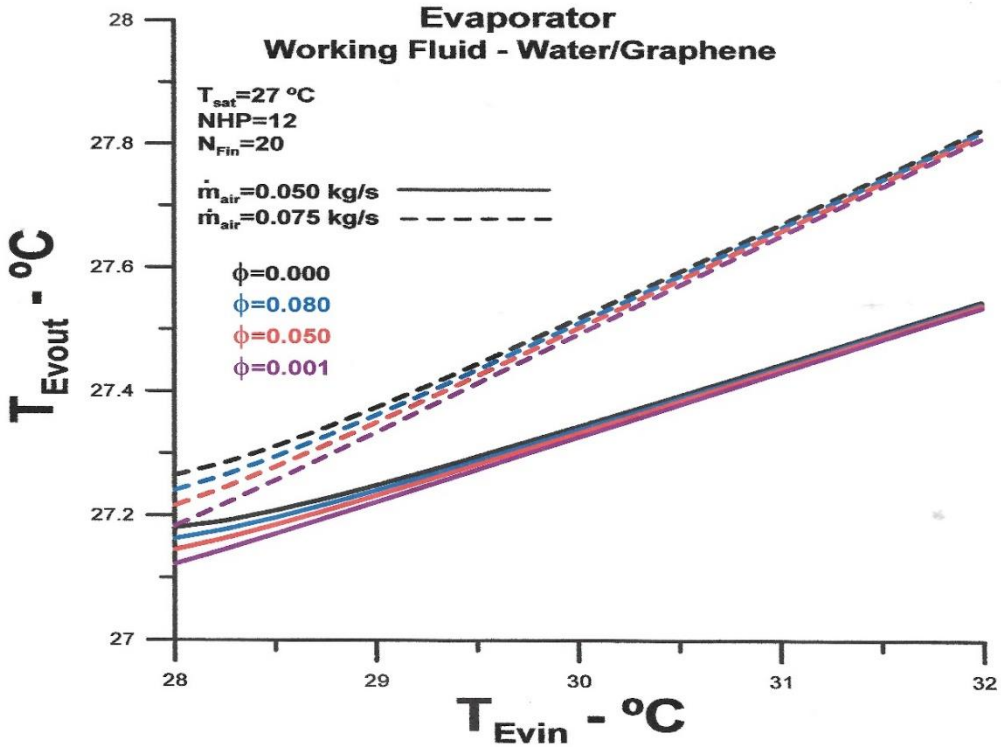

Figure 11: Outlet air temperature versus inlet air temperature for NHP=12 and N_{Fin}=20

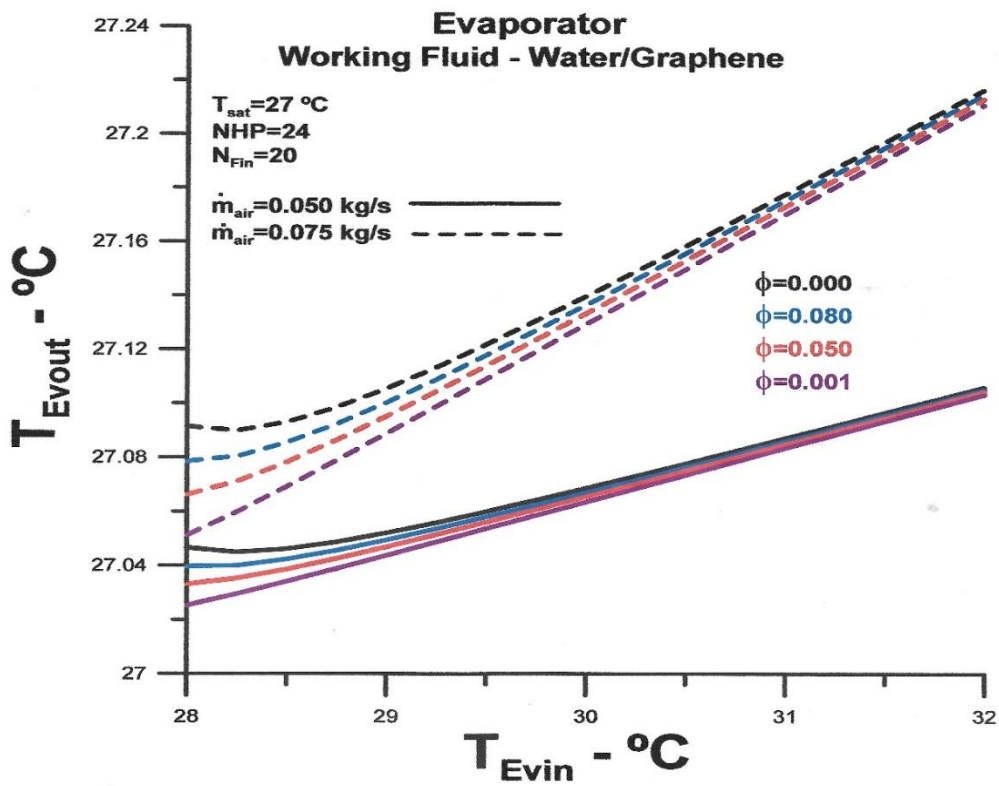

Figure 12: Outlet air temperature versus inlet air temperature for NHP=24 and N_{Fin}=20

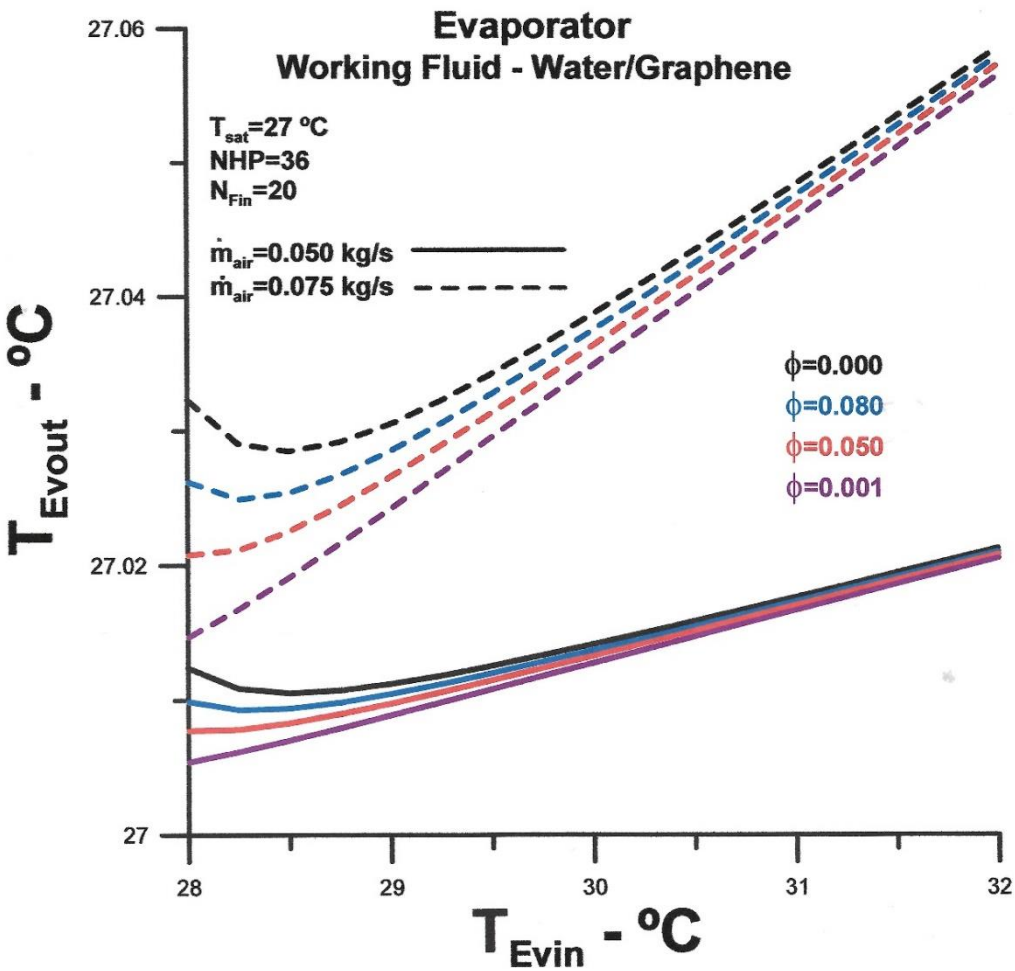

Figure 13: Outlet air temperature versus inlet air temperature for NHP=36 and N_{Fin}=20

CONCLUSION

The aim is to theoretically analyze the influence of the volume fraction of the nanofluid consisting of distilled water and graphene nanoparticles on the thermal performance of an evaporator made up of sets of heat pipes. The original evaporator uses distilled water as the working fluid and is part of a heat exchanger designed to work as an air conditioning system in operating rooms [1].

It is concluded that the nanofluid affects the heat exchange between the working fluid and the hot air entering the evaporator.

The most important conclusion of the performed analysis is that there is a volume fraction range for the nanofluid to work to improve the thermal performance of the heat exchanger. The results demonstrate that from a certain minimum value, there is greater heat exchange between the fluids until a certain volume fraction of the nanofluid is reached where the heat exchange is equal to the heat exchange of the original evaporator. Above this upper limit value in the volume fraction of the nanofluids, the heat exchange is lower than the heat exchange of the original evaporator.

According to the literature [1-15], many factors can lead to a high thermal resistance between the working fluid and the surface of the heat pipe, impairing the heat exchange. One is the deposition

of nanoparticles on the surface, and another, also feasible and related, is low pressure and the energy level involved in the process, that is, small heat exchangers are more affected.

REFERENCE

1. Ragil Sukarno, Nandy Putra1, Imansyah Ibnu Hakim, Fadhil Fuad Rachman, and Teuku Meurah Indra Mahlia (2021)." Multi-Stage Heat-Pipe Heat Exchanger for Improving Energy Efficiency of the HVAC System in a Hospital Operating Room." International Journal of Low-Carbon Technologies 2021, 16, 259–267. DOI:10.1093/ijlct/ctaa048

2. Nandy Putra, Trisno Anggoro, and Adi Winarta (2017). "Experimental Study of Heat Pipe Heat Exchanger in Hospital HVAC System for Energy Conservation." International Journal on Advanced Science Engineering and Information Technology Vol.7 (2017) No. 3. DOI: 10.18517/ijaseit.7.3.2135

3. Grzegorz Górecki, Marcin Łęcki, Artur Norbert Gutkowski, Dariusz Andrzejewski, Bartosz Warwas, Michał Kowalczyk and Artur Romaniak (2021). "Experimental and Numerical Study of Heat Pipe Heat Exchanger with Individually Finned Heat Pipes." Energies 2021, 14, 5317. https://doi.org/10.3390/en14175317

4. Hussam Jouhara, Sulaiman Almahmoud, Daniel Brough, Valentin Guichet, Bertrand Delpech, Amisha Chauhan, Lujean Ahmad, Nicolas Serey (2021). "Experimental and Theoretical Investigation of the Performance of an Air to Water Multi-Pass Heat Pipe-Based Heat Exchanger." Energy 219 (2021) 119624. https://doi.org/10.1016/j.energy.2020.119624

5. Khaled Elsaida, Mohamma Ali Abdelkareem, Hussein M. Maghrabie, Enas Taha Sayed, Tabbi Wilberforce, Ahmad Baroutaji, A.G. Olabi (2021). "Thermophysical Properties of Graphene-Based Nanofluids." International Journal of Thermofluids 10 (2021) 100073. https://doi.org/10.1016/j.ijft.2021.100073

6. Ali, N. (2022). "Graphene-Based Nanofluids: Production Parameter Effects on Thermophysical Properties and Dispersion Stability". Nanomaterials 2022, 12, 357. https://doi.org/10.3390/nano12030357

7. A. Kamyar, K.S. Ong, R. Saidur (2013). "Effects of Nanofluids on Heat Transfer Characteristics of a Two-Phase Closed Thermosyphon." International Journal of Heat and Mass Transfer 65 (2013) 610–618. http://dx.doi.org/10.1016/j.ijheatmasstransfer.2013.06.046

8. Agnieszka Kujawska, Robert Mulka, Samah Hamze, Gaweł Żyła, Bartosz Zajaczkowski, Matthias H. Buschmann, Patrice Estelle (2021). "The Effect of Boiling in a Thermosyphon on Surface Tension and Contact Angle of Silica and Graphene Oxide Nanofluids." Colloids and Surfaces A: Physicochemical and Engineering Aspects, Volume 627, 20 October 2021, 127082. https://doi.org/10.1016/j.colsurfa.2021.127082

9. Amir Akbari, Erfan Mohammadian, Seyed Ali Alavi Fazel, Mehdi Shanbedi, Mahtab Bahreini, Milad Heidari, and Goodarz Ahmadi (2019). "Comparison between Nucleate Pool Boiling Heat Transfer of Graphene Nanoplatelet- and Carbon Nanotube- Based Aqueous Nanofluids." ACS Omega 2019, 4, 19183−19192. DOI: 10.1021/acsomega.9b02474

10. Jacqueline Barber, David Brutin, and Lounes Tadrist (2011). "A Review on Boiling Heat Transfer Enhancement with Nanofluids." Nanoscale Research Letters 2011, 6:280. http://www.nanoscalereslett.com/content/6/1/280

11. K. N. Shukla A. Brusly Solomon, B. C. Pillai, and Mohammed Ibrahim (2010). "Thermal Performance of Cylindrical Heat Pipe Using Nanofluids." Journal of Thermophysics and Heat Transfer · October 2010. https://doi.org/10.2514/1.48749

12. Kapilan Natesan, Shashikantha Karinka (2023). "A Comprehensive Review of Heat Transfer Enhancement of Heat Exchanger, Heat Pipe and Electronic Components Using Graphene." Case Studies in The1mal Engineering 45 (2023) 10287 4. https:/ / doi.org/10.1 ol 6/ j.csite.2023.10287 4

13. Mohammed Salah Hameed, Abdul Rahman Khan, A. A. Mahdi (2013). "Modeling a General Equation for Pool Boiling Heat Transfer." Advances in Chemical Engineering and Science, 2013, 3, 294-303. http://dx.doi.org/10.4236/aces.2013.34037

14. A. Suriyawong, A. S. Dalkilic, and S. Wongwises (2012). "Nucleate Pool Boiling Heat Transfer Correlation for TiO2-Water Nanofluids." Journal of ASTM International, Vol. 9, No. 5. https://www.researchgate.net/publication/254200345

15. Nogueira, E. (2020). "Thermal performance in heat exchangers by the irreversibility, effectiveness, and efficiency concepts using nanofluids." Journal of Engineering Sciences, Vol. 7(2), pp. F1–F7. Doi: 10.21272/jes.2020.7(2).f1

16. Élcio Nogueira (2022). "Thermo-Hydraulic Optimization of Shell and Externally Finned Tubes Heat Exchanger by the Thermal Efficiency Method and Second Law of Thermodynamics." International Journal of Chemical and Process Engineering Research, 2022 Vol. 9, No. 1, pp. 21-41. DOI: 10.18488/65. v9i1.3130

17. Élcio Nogueira (2021). "Effects of R134a Saturation Temperature on a Shell and Tube Condenser with the Nanofluid Flow in the Tube Using the Thermal Efficiency and Effectiveness Concepts." World Journal of Nano Science and Engineering, 2021, 11, 1-24. https://doi.org/10.4236/wjnse.2021.111001

18. Warren M. Rohsenow (1951). "A Method of Correlating Heat Transfer Data for Surface Boiling of Liquids." Technical Report Nº 5, The Office Naval Research Contract N5ori-07827, Massachusetts Institute of Technology.